International Scientific Colloquium
Modelling for Material Processing
Riga, June 8-9, 2006

Design of an innovative heating process system for the epitaxial growth of silicon carbide layers wafer

M. Forzan, G. Maccalli, G. Valente, D. Crippa

Abstract

The epitaxial growth is a well-known technique to produce semiconductor wafers. In the paper, we will present how an innovative heating chamber (susceptor) for the epitaxial growth of Silicon Carbide at high temperature, has been designed.

The adopted solution to obtain a uniform temperature is to heat the silicon substrate inside an optical cavity, electrically heated by an external coil. The cavity is reproduced by two half moon-shaped conductive parts electrically insulated.

Numerical models have been applied to design the heating chamber and the inductor. In the paper, we will discuss our approach to model the system through 2D FEM magnetic models. These models also allowed to solve thermal analysis.

Electrical and thermal measurements performed on a prototype of the system will be also presented, allowing the validation of the FEM model. Comparisons between numerical and experimental results were made on the main electrical parameters (transferred power, power factor, quality factor) and on the differences of the predicted thermal profile and the experimental one.

1. General Information

Epitaxial growth is a well-known technique to produce semiconductor wafers. They are used to realize electronic power devices for converters (SCR, GTO, IGBT) and transistor microcircuits, widely involved in data processing and storage.

LPE® and ETC® are two outstanding designer and manufacturer of induction heating plants for the epitaxial growth of doped layers on silicon crystal. In the paper, it is presented how an innovative heating chamber (susceptor), that allows the epitaxial growth on SiC at high temperature, has been designed. The main goal for the electrical designer is to reach a certain temperature distribution inside the silicon carbide slice.

The best solution to obtain a uniform temperature is to create an optical cavity electrically heated by eddy currents induced by an external coil. That cavity has been realized with two *half moon-shaped* conductive pieces electrically independent, separated by two side walls thermally, but not electrically conductive. The heating chamber is made of pure graphite, a good electrical conductor. The two side walls are made of sintered silicon carbide, which is a good electrical insulator and thermal conductor. The external cylinder is the thermal insulation of the

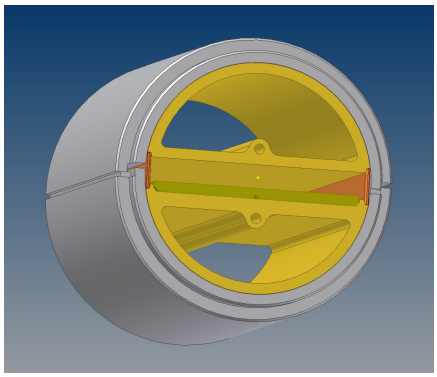

Fig.1: The heating chamber with the external porous graphite.

inner part of the system. It is made of porous graphite that is a poor electrical and thermal conductor.

Numerical models have been applied to design the heating chamber and the inductor. In the paper, we will discuss our approach to model the system through 2D and 3D FEM magnetic models coupled with electrical circuits. Magnetic models also allowed us to solve the thermal analysis to verify the final thermal profile.

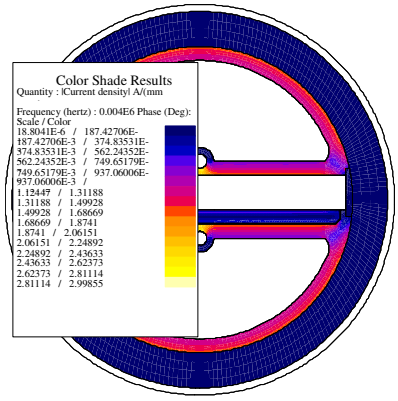

Fig.2: Eddy current density in 10mm thick susceptor graphite.

2. Numerical models

The design of the heating chamber has been carried out through several steps. The initial investigations have been devoted to the geometric design of the system; the optimal thicknesses of the different layers (internal graphite, the insulating layer etc) have been determined through a 2D analysis where currents flow on the model plane and magnetic fields are normal to the plane. The formulation adopted for this kind of problem, known in literature as H formulation, can be derived from Maxwell's equation and can be written in a steady state regime:

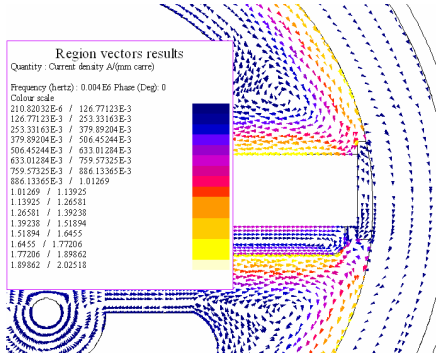

Fig.3: Eddy current vector field and density in 30mm thick susceptor graphite.

$$\nabla^2 \overline{H}_Z - j\omega\sigma\mu\overline{H}_Z = 0 \qquad (1)$$

where $\overline{H}_Z$ is the phasor of the component normal to the model plane of the magnetic field, ω the angular frequency, σ the electrical conductibility, μ the magnetic permeability. The solution of homogeneous Helmoltz's equation can be obtained setting Dirchlet's conditions for the H field on the external boundary of the model. The current density distribution can be computed from Ampere's Law.

The design of the inductor have been developed also through 2D FEM models, considering an axial cross section of the system. In this case, the geometry can be simplified considering an axi-symmetric system where the magnetic field has radial and axial components and the current density is normal to the plane. The FEM solution of this problem can be obtained using the vector potential A coupled with the scalar electric one, V. In 2D, the vector potential has only the azimuthal component and consequently the equation to be solved is:

$$\nabla \times \frac{1}{\mu}\left(-\frac{\partial \overline{A}_\phi}{\partial r}\vec{u}_r + \frac{1}{r}\frac{\partial r\overline{A}_\phi}{\partial r}\vec{u}_z\right) + j\omega\sigma r\overline{A}_\phi - \nabla V = 0 \qquad (2)$$

where $\overline{A}_\phi$ is the phasor of the azimuthal component of the vector magnetic potential, V is the scalar electric potential.

The solution of (2) can be achieved using Galerkin's method (weighted residual): using this solving method, the solution can be directly coupled to an external circuit. The state variable of the FE problem, the vector potential, can be directly coupled to the circuit equation:

$$\sum_j \left(M_{i,j} + j\omega L_{i,j}\right)A_j - \sum_{r=1}^{Tsol} R_{i,q}V_{sol,q} = 0 \qquad (3)$$

where:

$$M_{i,j} = \int_{\Omega} \frac{\nabla N_i \nabla N_j}{\mu} d\Omega; \quad L_{i,j} = \int_{\Omega} \sigma N_i N_j d\Omega; \quad R_{i,q} = \int_{\Omega sol,q} \frac{\sigma}{l} N_i d\Omega \tag{4}$$

and N_i is the shape function related to the node i, T_{sol} is the number of solid conductors, $V_{sol,q}$ is the voltage drop and $\Omega_{sol,q}$ is the cross-section of solid conductor q. The total current through a solid conductor can be expressed in the following form:

$$I_{sol,q} = \frac{\sigma \Omega_{sol,q}}{l} V_{sol,q} - j\omega l \sum_j R_{j,q} A_j \tag{5}$$

Taking into account this expression the FE-circuit matrix can be assembled in the following way:

$$\begin{bmatrix} M_{i,j} & -R_{i,q} \\ -j\omega l R_{i,q} & \frac{\sigma \Omega_{sol,q}}{l} \end{bmatrix} \cdot \begin{bmatrix} A_j \\ V_{sol,q} \end{bmatrix} = \begin{bmatrix} 0 \\ I_{sol,q} \end{bmatrix} \tag{6}$$

We applied the external circuit to take into account that the real geometry of the device is not axisimmetric due to the presence of a transverse path where the current induced into the graphite region flows. The presence of transverse paths modifies the intensity of the induced current: this effect has been described closing the graphite region into an external resistance. The value of this resistance has been chosen to fit the results obtained on a 3D model where the transverse paths have been modelled. The inductor design must satisfy several requirements, but we focused the attention to the power density induced inside the graphite. The goal was to reach a given power distribution in order to create the temperature profile that allows the epitaxial growth of silicon carbide. The 2D axisimmetric model is obviously faster than a complete 3D model, so a numerical parametrical analysis with several different inductor configurations have been done in a reasonable time.

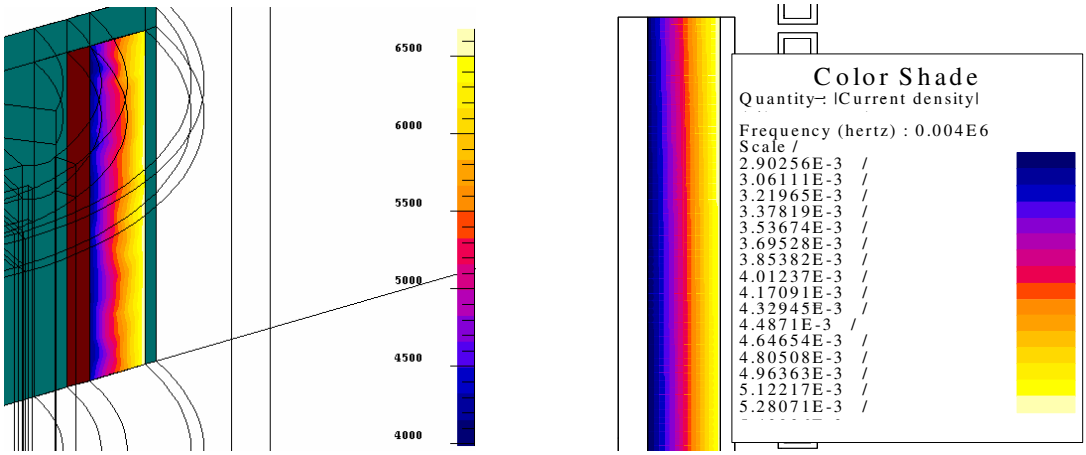

Fig.4: Comparison between the 3D model and the 2D one coupled with an external circuit

For this scope, it has been estimated the distribution of power losses in the graphite cell. It can be subdivided into four components of heat exchange: convection with process gases, radiation through input and output cell openings, radiation and convection through external surface of insulating layer. The values of all the losses depend upon the cell temperature *T*: it is supposed to be uniform in the whole cell and equal to 1800°C, in steady state condition. We assumed the convection coefficient *hest* equal to 10W/m^2/K and the thermal conductivity of the insulating layer equal to 29W/m^2/K, according to the manufacturer datasheet. Power losses by convection with the external air at the temperature *Test* resulted in 2.3kW, and radiated heat from the external surface *Sfes* of insulation resulted in 11.7kW, being the external insulation layer at the temperature *Tp* 580°C. We considered all these losses

as uniform in the cell. On the contrary the heat exchange with the gases *Qgas* varies along the cell, because the temperature of process gases is dependent on the axial position. The radiated heat through cell openings *S* depends upon the axial position, because the view factor depends on the distance from the openings [4]. All the thermal losses previously described contribute to the thermal equilibrium as in the following:

$$Q = hest \cdot S \cdot (Tp - Test) + \sigma \cdot \varepsilon \cdot S \cdot \left[(Tp + 273)^4 - (Test + 273)^4\right] + \\ + \sigma \cdot \varepsilon \cdot Sfes \cdot \left[(T + 273)^4 - (Test + 273)^4\right] + Qgas \quad (7)$$

where σ is the Boltzmann constant, ε is the emissivity, and the view factor has been estimated to 1, instead of the exact value 0.87, the total amount of power to be transferred in the graphite is 30kW.

To reproduce axial variations, in the electro-thermal FE model, we subdivided the cell into 6 transverse stripes equally spaced, each of them with a proper heat exchange coefficient, which summarize all kind of heat exchange in the particular region. To consider also the internal reflections in the *half moon* cavities, between the sections of graphite parts in the 2D model, we introduced a fictitious material with very high thermal conductivity. Finally, to reproduce a non axi-symmetric geometry into an axi-symmetric one, the position of the transverse path has been properly modified.

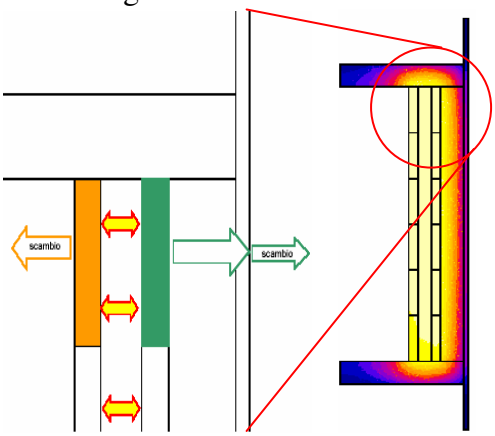

Fig.5: Thermal model with some general results

3. Experimental results

3.1. Circuital equivalent parameters (parallel configuration)

All main electrical parameters computed with simulations have been compared with measures from the experimental activities.

Being impossible, on the built apparatus, to directly measure the equivalent impedance of the whole system inductor-susceptor, we deducted the values of the equivalent integral parameters in an indirect way.

System inductance is calculated starting from well-known values of the resonance frequency and the capacitance of the tank circuit. Existing differences between measured values and computed values depends upon the different tank circuit frequency, not exactly reproduced in the real application. The equivalent resistivity of the whole system is calculated on the base of active power, the output of the frequency converter, measured by instruments installed in the DC section of the converter itself. Data listed in Table 1 show a considerable difference between the value of the total equivalent resistance of the test apparatus computed in the FE model and the measured one. This fact can be explained because the model considers external fictitious resistances, introduced in the external

Parallel configuration	**Simulation**		**Measure**	
	Rump up	*Steady state*	*Rump up*	*Steady state*
Tank Circuit Frequency	4000 Hz	4000 Hz	5343 Hz	5330 Hz
Tank Circuit Capacitance	/	/	62.4 µF	62.4 µF
Tank Circuit Inductance	18.4 µH	18.1 µH	21.0 µH	21.2 µH
Generator Inductance	/	/	44 µH	44 µH
Total Active Power	41 kW	29 kW	40 kW	29 kW
Total Resistance	6.13 Ω	6.36 Ω	2.61 Ω	2.45 Ω

Table 1: Circuital equivalent parameters

circuit to take into account the transverse path and the couple of cuts in the external insulating layer (this in particular, overestimated).

Finally, the good correspondence between the expected total power to the load and the estimated one, confirms the goodness of the thermal model and of the preliminary evaluations of power losses, presented in §3.

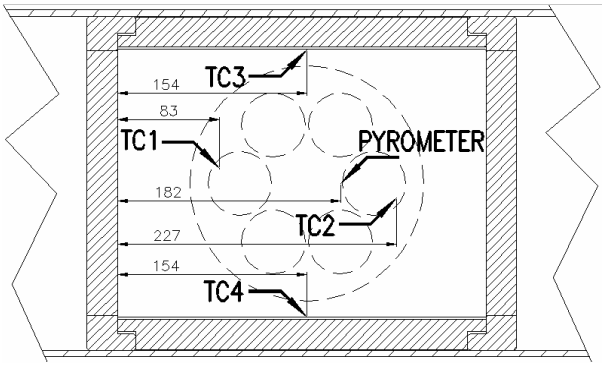

Fig.6: Probes positions in the flat part of the upper half moon graphite part, with dashed the image of the faced susceptor below

3.2. Temperature profile

Technical solution to achieve the goal must satisfy two requirements. First of all, the heart of the heating system, the susceptor which contains SiC substrates, is located in the lower graphite *half moon* part of the chamber, and is electrically isolated from the other graphite parts, being floating on a gas cushion. This implies that Joule effect due to eddy currents in the susceptor is not enough to heat substrates up to the required temperature. Only the power radiated from transverse path of the cell can bring to the expected temperature the susceptor. For this reason the goal of the project evolved toward the design of quasi-optical cavity in which the temperature is supposed to be almost uniform. This is the second input for the project development. The main scope of the authors was the design of a reaction chamber with a well defined temperature axial profile, in order to guarantee the expected chemical reactions kinetics. This profile should be as uniform as possible in correspondence of the susceptor.We used an optical monochromatic pyrometer and four thermocouples C-Type W5Re/W26Re, capable to read temperature up to 2320°, to measure the temperature in different zones of the reaction chamber. Being impossible to take direct temperature measure on the susceptor surface, because of the particular geometry of the described cell, thermocouples and pyrometers were used to get data

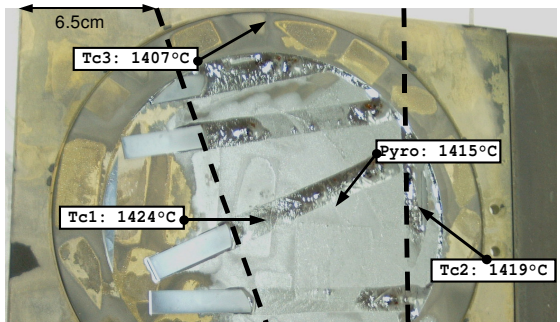

Fig.7: Silicon pieces melted on the susceptor. Test to compare susceptor temperature and probes measures. For this test probes positions have been changed as shown in the present picture.

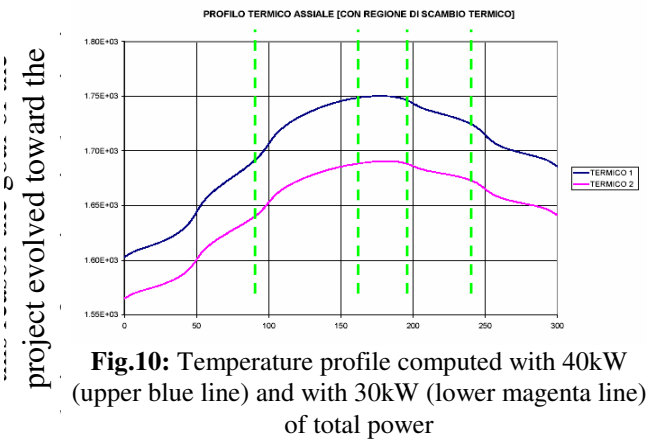

Fig.10: Temperature profile computed with 40kW (upper blue line) and with 30kW (lower magenta line) of total power

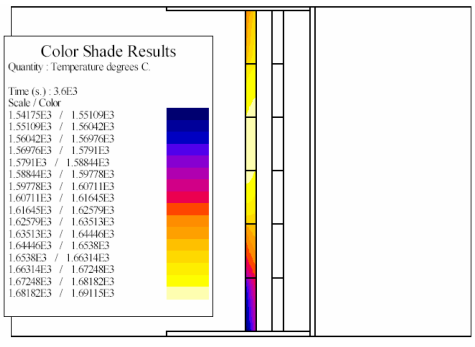

Fig.11: Thermal status computed in case of 30kW to the load

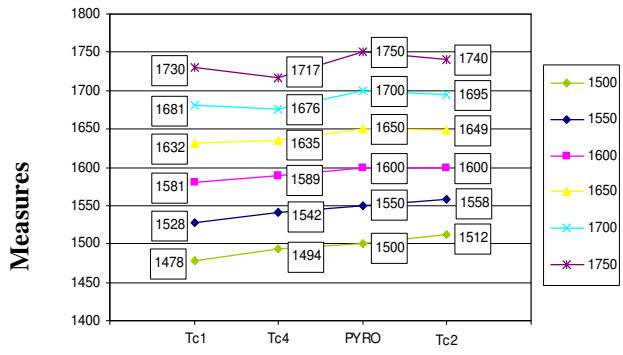

Fig.8: Temperature profile measured above the susceptor in the points shown in Fig. 6

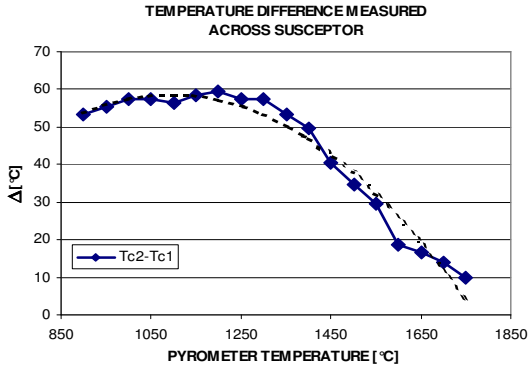

Fig.9: Temperature difference across the susceptor versus T-Pyro

on the thermal status of the flat part of the upper *half moon*. In fact the thermal graphite conductivity and the low thickness of the cell compared to the penetration depth of magnetic field, lead to a uniform temperature across the whole thickness of graphite in any section of the cell and, in particular, where heat exchanges with gases are lower, i.e. above the susceptor. In a steady state thermal regime there is an equilibrium in radiated power exchange inside the cell, so you can expect to have on the transverse path a good image of the thermal status of the susceptor. To validate these assumptions and also to check instruments calibration, we made tests melting silicon stripes on a dummy susceptor at the temperature of 1415°C, as read with the pyrometer.

The thermal status of the susceptor can be deducted from the melted zone of the silicon strips, as shown in Fig.7. Results confirm the goodness of preliminary assumptions. For this reason, data listed in Table 2 are an accurate image of the thermal status on the susceptor. The comparison between measures and computation shows a good accordance of results from FE electro-thermal model with the real apparatus. In Fig.8 it is shown a diagram where are represented temperature measured by Tc1, Tc2, Tc4 and pyrometer, which trend fits well with the temperature profile computed in the FE model shown in the diagram of Fig.10. In proximity of 1700°C, differences between Tc2 and pyrometer are in the order of 10°C, just like in thermal simulation (magenta line in Fig.10). More considerable is the difference between Tc1 measure and the expected value. But, taking into account that the accuracy of thermocouples is ±1%, the difference of 20°C between the expected and the measured value can be considered negligible. So the real temperature profile profile along the susceptor region is really well fitted by the simulation. We must also underline that, for higher temperature, according to pyrometer measure, differences between the FE model results and the real apparatus, are larger. This is a consequence of a limit of the thermal model applied where all the coefficients describing convection and radiation are fitted for a given temperature, 1650°C. To solve this problem, as above-mentioned, we filled cavities in the graphite *half moon* had been filled with a fictitious material with very high thermal conductivity, as to compensate radiation in the cavities with conduction. Radiation is proportional to the fourth power of temperature difference, conduction is a linear function of the temperature difference across a medium. Being the thermal model calibrated for 1650°C, away from this temperature, the approximation of the model is worse and worse.

4. Conclusions

The problem to design a heating chamber with high performances in temperature uniformity has been analysed and solved in such an innovative way to be patented by ETC®

company. Two graphite crucibles resulted a good approximation of an optical cavity, when they are electrically, but not thermally isolated each other. Thanks to appropriate preliminary physical considerations regarding the electrical and the thermal behaviour of the system, a very good approximation of the real apparatus has been implemented in the FE model, either in the electromagnetic one, either in the electro-thermal one.

References

[1] H. De Gersem, R. Mertens, U. Pahner, R. Belmans, K. Mameyer: A Topological Method used for Field-Circuit Coupling, IEEE Trans. On Mag. Vol. 34, No 5, Sept. 1998.

[2] K.J.Binns, P.J.Lawreson, C.W.Trowbridge: The Analytical and Numerical Solution of Electric and Magnetic Field, John Wiley and Sons, Chichester, 1992.

[3] Cedrat, Flux User's Guide, Meyland, France

[4] Y. A. Çengel: Heat Transfer – A Practical Approach, WCB/Mc Graw Hill, New York, 1998.

Authors

Michele Forzan PhD Researcher in Università di Padova, Electrical Engineering Dept.

Giacomo Maccalli, LPE Epitaxial Technology Project Engineer, PhD Student at the Politecnico di Milano, Electrical Engineering Dept.

Gianluca Valente PhD, LPE Epitaxial Technology R&D Dept.

Dott. Danilo Crippa, LPE Epitaxial Technology R&D Manager.